

# Investigation on Behaviour of Cold-Formed Ferritic Stainless Steel Hollow Beams

M. Nilakanmani<sup>1</sup> and M. Anbarasu<sup>2</sup>

<sup>1</sup>PG Student, <sup>2</sup>Assistant Professor, Department of Civil Engineering,  
Government College of Engineering, Salem, Tamil Nadu, India  
E-Mail: nilakanmani@gmail.com, gceanbu@gmail.com

**Abstract** - This work deals with the investigation on the behavior of cold-formed ferritic stainless steel hollow beams. The numerical model was developed by using Finite Element (FE) software ABAQUS [1]. The developed FE model includes material non-linearity, geometric non-linearity and geometric imperfections. The numerical model is validated by comparison of experimental results reported by Afshan and Gardner (2013) [2]. The sections for parametric study were selected based on the EN-1993-1-4 specifications [8]. The key parameters varied in the study were material properties, section geometry and thickness of the section. The parametric study has been carried out by using the verified FE model and the results were compared with the flexural resistance predicted by the Direct Strength Method (DSM) [3]. Based on the comparison of results the effect of geometric parameters on the cold-formed ferritic stainless steel hollow beams are discussed and based on the comparison of results the possible conclusions are drawn.

**Keywords:** Abaqus, Beams, Direct Strength Method, Ferritic Stainless Steel, Hollow Section

## I. INTRODUCTION

STAINLESS steel is classified into five main categories: ferritic, austenitic, martensitic, duplex and precipitation hardening. Out of which, austenitic and duplex have been widely used in structural applications in construction industry. Ferritic stainless steel differs from other grades, having a low content of nickel offers a more appropriate balance of properties for structural applications and material cost. Ferritic stainless steel possesses many advantages that austenitics have over carbon steel but at lower material cost. These steels are easier to work and machine than the austenitic grades and have a higher yield strength in annealed condition [4]. They are also widely used in automotive industry, road and rail transport, power generation and mining. However, its structural application remained relatively scarce.

Theofanous and Gardner (2010) [15] studied the load bearing and deformation capacity of Lean Duplex Stainless Steel (LDSS) hollow section beams and concluded that the continuous strength method (CSM) has been found to provide better estimates of the ultimate moment resistance of LDSS beams. Afshan and Gardner (2013) [2] conducted laboratory testing on ferritic stainless steel Grades EN 1.4003 and EN 1.4509 on hollow sections. They concluded that current Class 3 slenderness limits provided in EN 1993-

1-4 (CEN 2006a) [8] is applicable to ferritic stainless steel internal elements under compression and Class 2 limit of EN 1993-1-4 [8] (CEN 2006a) was considered to be safe. Bock et al. (2014) [6] analysed and assessed the predictive expression given in Annex C of EN 1993-1-4 [8] for ultimate strain  $\epsilon_u$  using numerical results. They concluded that current predictive model is appropriate for ferritics and yields unconservative results and CSM predictions are more accurate and consistent. Bock et al. (2015) [5] assessed the adequacy of slenderness limits and effective width formula given in EN 1993-1-4 [8] to ferritic stainless steels with experimental results, and those proposed by other researchers design approach [9] with the obtained test results. Tao and Rasmussen (2016) [14] studied ferritic stainless steels of different mechanical properties and developed revised models for flat material and corner material of cold-formed ferritic stainless steel hollow sections with a yield stress ranging from 250 to 550 MPa.

This work reports the results of buckling behavior of cold-formed ferritic stainless steel hollow beams. The numerical model was developed by using Finite Element (FE) software ABAQUS [1] and the results were verified with the experimental results reported in the literature [2]. Followed by the parametric study by varying the section geometry, thickness and 0.2% proof strength of steel. The beams considered for the parametric study includes the hollow beam with uniform bending under ideal simply supported boundary condition. The results were used to check the applicability of the DSM (AISI-S100:2012) [3] for cold-formed ferritic stainless steel hollow beam sections.

## II. FINITE ELEMENT MODELLING

The FE software ABAQUS 6.13 (2013) [1] was used to simulate the numerical model of cold-formed ferritic stainless steel hollow beams. The developed FE model includes the material non-linearity, geometric non-linearity and local geometric imperfections [13]. The nonlinear behaviour of stainless steel was introduced into ABAQUS by defining a multi-linear stress-strain curve based on the revised Tao and Rasmussen (2016) [14] material model. Each specimen is divided into three parts as tensile flat (TF), compressive flat (CF) and tensile corner (TC) portion [15] as shown in Fig. 1.

The strain hardening characteristics of cold-formed ferritic stainless steel was also included by assigning TC property to extended distance equal to two times the material thickness into the flat region of each face in addition to the curved portion as suggested by Theofanous and Gardner (2010) [15].

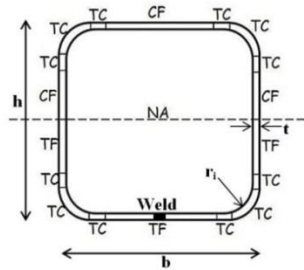


Fig. 1 Material Properties Assigned to the Various Parts of the Cross-Sections

The mesh size was equal to thickness of the element for the flat elements, while the curved geometry of corner regions was approximated by 3 elements as suggested by Bock *et al.*

(2014) [6]. The element used for modeling was a four-noded doubly curved shell with reduced integration (S4R) from the ABAQUS element library [10], [12].

The end cross-sections of the beams were constrained to remain undeformed using kinematic coupling, and translation along the x, y and z direction are restrained along with the rotation along the z-direction at hinged end. At the roller end, the same end condition prevails except the translation along the z-direction. The loads were applied at the load points at the junction of the web with the corner radius in the lower (tension) part of the beam to avoid web crippling as suggested by Theofanous and Gardner (2010) [15] to simulate 4-point bending and 3-point bending.

Linear buckling analysis is done to obtain buckling load and buckling modes. In non-linear analysis, load control analysis was done with static riks step. The measured dimensions and material properties for the validated sections are shown in Table I and Table II respectively [2].

TABLE I MEASURED DIMENSIONS OF THE BEAM SPECIMENS

S. No.	Specimen ID	L	H	B	t	r <sub>i</sub>	w <sub>o</sub>
		mm	mm	mm	mm	mm	mm
1	120x80x3-4PB	1500	120.0	79.9	2.84	3.78	0.061
2	80x80x3-4PB	1500	80.4	80.0	2.80	3.95	0.087
3	60x60x3-4PB	1500	60.7	60.7	2.89	2.86	0.061
4	120x80x3-3PB	1500	119.9	79.9	2.83	3.80	0.061
5	60x40x3-3PB	1500	60.4	40.8	2.82	3.18	0.081
6	80x80x3-3PB	1500	80.5	80.2	2.81	3.81	0.087
7	60x60x3-3PB	1500	60.6	60.5	2.87	2.88	0.061

TABLE II MATERIAL PROPERTIES OF TEST SPECIMENS

Material properties	Specimen ID	E	$\sigma_{0.2}$	$\sigma_{1.0}$	$\sigma_u$	n
		N/mm <sup>2</sup>	N/mm <sup>2</sup>	N/mm <sup>2</sup>	N/mm <sup>2</sup>	
Tensile Flat (TF)	120x80x3	216000	423	-	472	10.2
	60x40x3	219300	454	-	475	7.8
	80x80x3	210000	431	-	447	8.7
	60x60x3	218300	519	-	534	7.8
Compression Flat (CF)	120x80x3	211150	404	451	-	5.8
	60x40x3	217200	417	475	-	6.4
	80x80x3	211250	404	456	-	6.3
	60x60x3	215130	483	531	-	6.3
Tensile Corner (TC)	120x80x3	226000	535	-	554	6
	60x40x3	200000	545	-	597	4.7
	80x80x3	220000	512	-	520	7.8
	60x60x3	225000	580	-	665	4.3

#### A. Validation

The numerical model was validated by means of comparison with the experimental results reported by

Afshan and Gardner (2013) in terms of variation of moment capacities and non-dimensional moment versus rotation curve  $[(M/M_{PL}) \text{ Vs } (\theta/\theta_{PL})]$ . The comparison between the ultimate moment of the tested specimens and those

computed by the finite element analysis are presented in Table III. The variations of non-dimensional moment versus rotation curve  $[(M/M_{PL}) \text{ Vs } (\theta/\theta_{PL})]$  for 120x80x3-3PB is presented in Fig. 2 and found reasonable agreement with each other.

TABLE III COMPARISON OF  $M_{EXP}$  AND  $M_{FEA}$

S. No.	Specimen ID	Ultimate load (kNm)		$(M_{EXP}) / (M_{FEA})$
		$M_{FEA}$	$M_{EXP}$	
1	120x80x3-4PB	20.000.0	20.42	0.97
2	80x80x3-4PB	11.30	11.14	1.01
3	60x60x3-4PB	7.90	8.26	0.96
4	120x80x3-3PB	21.10	20.65	1.02
5	60x40x3-3PB	5.90	5.83	1.01
6	80x80x3-3PB	11.40	11.44	0.99
7	60x60x3-3PB	8.40	8.13	1.03
Mean				0.99
Standard Deviation				0.026

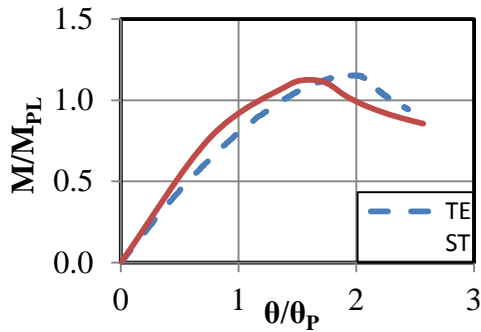


Fig. 2  $[(M/M_{PL}) \text{ Vs } (\theta/\theta_{PL})]$  for 120x80x3-3PB

### III. PARAMETRIC STUDY

Having validated the FE model, further numerical analyses were conducted to generate results over a wide range of section geometries and slendernesses. The objective of the parametric study is to study the factors governing local buckling behaviour of the cold-formed ferritic stainless steel hollow beams subjected to uniform bending about major axis under ideal simply supported boundary condition. A total of 20 FE models of ferritic stainless steel SHS with three different cross-sections of 50 X 50, 100 X 100 and 150 X 150 (all in mm), beam lengths of 900 mm and 1500 mm and thickness varying from 1 mm to 5 mm, with (b/t) ratio varying from 16 to 96 were analyzed in the FE package ABAQUS [1]. The section dimensions were selected based on European standards (EN-1993-1-4) [8],[7]. The FE models of the ferritic stainless steel hollow beams were based on the center line dimensions of the cross-sections together with the plate thickness. Two different material properties for Ferritic grade 1.4003 stainless steel were obtained from the results reported by Afshan and Gardner (2013) [2]. Specimen labeling for the sections were done as shown in Fig. 3.

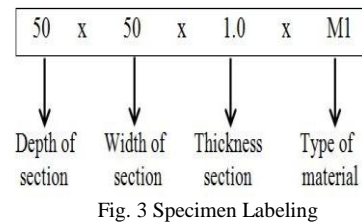


Fig. 3 Specimen Labeling

Table IV shows the material properties for the tensile flat (TF), compressive flat (CF) and tensile corner (TC) portions.

TABLE IV MATERIAL PROPERTIES FOR THE SECTIONS STUDIED

Material Property		E	$\sigma_{0.2}$	$\sigma_{1.0}$	$\sigma_u$	$\epsilon_f$	n	n'
		N/mm <sup>2</sup>	N/mm <sup>2</sup>	N/mm <sup>2</sup>	N/mm <sup>2</sup>	%		
M1	TF	216000	423	-	472	34	10.2	4.9
	CF	211150	404	451	-	-	5.8	3.1
	TC	226000	535	-	554	13	6	-
M2	TF	218300	519	-	534	16	7.8	10.8
	CF	215130	483	531	-	-	6.3	3.1
	TC	225000	580	-	665	13	4.3	9.5

The deformation shape for the section 50x50x1.0xM1 obtained from non-linear analysis is shown in Fig. 4. The results and discussion is presented below. Fig. 5 shows the relationship between the normalized ratio (b/t) and the normalized ratio ultimate moment to the yield moment of the beam ( $M_{FEA}/M_y$ ) for the different cross sections studied. From the figure it is observed that ( $M_{FEA}/M_y$ ) ratio increases with decrease in b/t ratio. Because of the increasing (b/t) ratio leads to the occurrence of local buckling of the cross section in the compression zone.



Fig. 4 Deformation shape for the section 50x50x1.0xM1

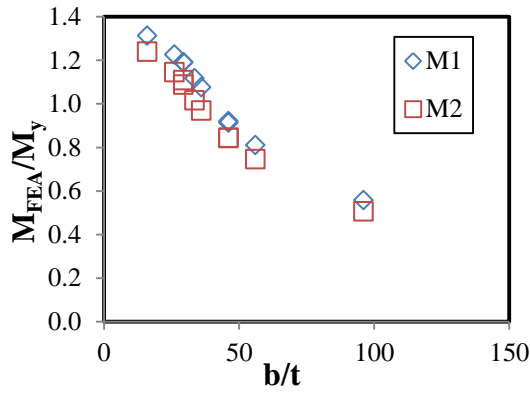


Fig. 5 Relationship between  $b/t$  and  $M_{FEA}/M_y$  for different cross sections

**A. Direct Strength Method (DSM)**

In general, the DSM is better than effective width method in terms of easy calculation, better results and time saving. Hence DSM is used in this study of cold-formed ferritic stainless steel hollow beams, was based on 1.2.2 of Appendix 1 in the North American Specification for the Design of Cold-Formed Steel Structural Members [3].

The nominal flexural strength ( $M_{DSM}$ ) shall be determined by the minimum of the nominal flexural strength for lateral-torsional buckling resistance ( $M_{ne}$ ), local buckling resistance ( $M_{nl}$ ), and distortional buckling resistance ( $M_{nd}$ ). Distortional buckling did not occur for closed hollow beams. Out of 20 sections studied, only 11 sections failed by local buckling in DSM and remaining sections failed by lateral torsional buckling. The sections having ( $b/t$ ) ratio above 36 and 33.50 failed by local buckling for M1 and M2 respectively.

However, the DSM in the current specifications (AISI-S100:2012) does not cover the design of cold-formed ferritic stainless steel hollow sections. The structural behavior of cold-formed ferritic stainless steel hollow sections could be quite different from the cold-formed singly symmetric open steel sections based on which the current DSM equations were developed. Hence, the

appropriateness of the DSM on the cold-formed ferritic stainless steel hollow sections subjected to bending was evaluated. Using CUFSM software geometric properties and elastic instabilities for the gross section were found.

The mean value of FEA-to-predicted moment ratio ( $M_{FEA}/M_{DSM}$ ) is 1.12 with the corresponding standard deviation of 0.074. The comparison of FEA results with DSM strengths are plotted in Fig. 6. It is shown that the current DSM predictions are conservative for the cold-formed ferritic stainless steel hollow section beams.

**IV. CONCLUSION**

Numerical and theoretical investigation on the structural performance of cold-formed ferritic stainless steel hollow flexural members has been presented in this paper. A FE model of flexural members was developed and verified by comparison of experimental results reported by Afshan and Gardner (2013) in terms of moment capacities and non-dimensional moment versus rotation curve [ $(M/M_{PL})$  Vs  $(\theta/\theta_{PL})$ ] using FE software ABAQUS. Having validated the FE model, further numerical analyses were conducted with wide range of section geometries, slendernesses and with two different types of material model. Then the numerical results were compared with the design strength predicted by the DSM. In DSM, only 11 sections out of 20 failed by local buckling. Finally, based on the comparison of results, the following conclusions are drawn

1. The impact of changing geometric parameters on the cold-formed ferritic stainless steel hollow beams,  $M_{FEA}/M_y$  ratio increases with decrease in  $b/t$  ratio of the flange.
2. Comparison of results for different cross sections with varying thickness, the cross sections with ( $b/t$ ) ratio above 36 and 33.50 fail by local buckling for Material 1 (M1) and Material 2 (M2) respectively
3. Based on the comparison of results between finite element analysis and DSM, DSM results are conservative for the sections studied.

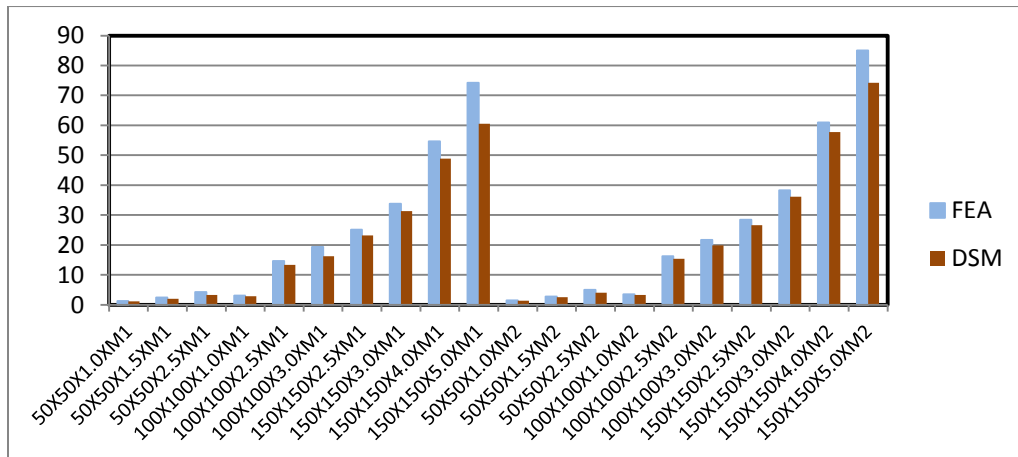


Fig. 6 Comparison of FEA results with DSM strengths

## V. NOTATION

The following symbols are used in this paper

$b$	-	Flat width of the beam
$t$	-	Thickness of the beam
$r_i$	-	Internal radius of corner at top and bottom
$w_o$	-	Local imperfection
$L$	-	Length of the beam
$H$	-	Height of the beam
$B$	-	Width of the beam
$E$	-	Young's modulus
$\sigma_{0.2}$	-	0.2% proof stress
$\sigma_{1.0}$	-	1.0% proof stress
$\sigma_u$	-	Ultimate stress
$\epsilon_u$	-	Ultimate strain
$\epsilon_f$	-	Tensile strain at fracture
$n, n'$	-	Strain hardening exponent
$M$	-	Moment of the section (kNm)
$M_{PL}$	-	Plastic Moment (kNm)
$\theta$	-	Rotation (rad)
$\theta_{PL}$	-	Rotation corresponding to plastic moment (rad)
$M_{EXP}$	-	Moment capacities obtained from experimental investigation
$M_{FEA}$	-	Moment capacities obtained from FE Analysis
$M_{DS}$	-	Moment capacities obtained from Direct Strength Method
$M_{nl}$	-	Local buckling resistance
$M_{nd}$	-	Distortional buckling resistance
$M_{ne}$	-	Lateral-torsional buckling resistance
$M_y$	-	Moment causing initial yield

## REFERENCES

- [1] ABAQUS, Dassault Systems Simulia Corp, ABAQUS Standard User's Manual Version 6.13, USA, 2013.
- [2] S. Afshan and L. Gardner, "Experimental Study of Cold-Formed Ferritic Stainless Steel Hollow Sections", 10.1061/ (ASCE) ST.1943-541X.0000580, 2013.
- [3] AISI-S100:2012, North American Specification for the Design of Cold-Formed Steel Structural Members specification, Washington, DC, USA.
- [4] I. Arrayago and E. Real, "Experimental study on ferritic stainless steel simply supported and continuous beams", *Journal of Constructional Steel Research*, Vol. 119, pp. 50-62, 2016.
- [5] M. Bock, I. Arrayago and E. Real, "Experiments on cold-formed ferritic stainless steel slender sections", *Journal of Constructional Steel Research*, Vol. 109, 13-23, 2015.
- [6] M. Bock, L. Gardner and E. Real, "Material and local buckling response of ferritic stainless steel sections", *Thin-Walled Structures*, Vol. 89, 131-141, 2014.
- [7] EN 1993-1-3, Eurocode 3: Design of steel structures - Part 1-3: General rules - Supplementary rules for cold-formed members and sheeting, 2006.
- [8] EN 1993-1-4, Eurocode 3: Design of steel structures - Part 1-4: General rules - Supplementary rules for stainless steels, 2006.
- [9] L. Gardner and M. Theofanous, "Discrete and continuous treatment of local buckling in stainless steel elements", *Journal of Constructional Steel Research*, Vol. 64, No. 11, pp. 1207-1216, 2008.
- [10] Y. Huang and B. Young, "Experimental and numerical investigation of cold-formed lean duplex stainless steel flexural members", *Thin-Walled Structures*, Vol. 73, pp. 216-228, 2013.
- [11] S. Niu, K. J. R. Rasmussen and F. Fan, "Distortional-global interaction buckling of stainless steel C-beams: Part I: Experimental investigation", *Journal of Constructional Steel Research*, Vol. 96, pp. 127-139, 2014.
- [12] S. Niu, K. J. R. Rasmussen and F. Fan, "Distortional-global interaction buckling of stainless steel C-beams: Part II: Numerical study and design", *Journal of Constructional Steel Research*, Vol. 96, pp. 40-53, 2014.
- [13] J. K. Sonu and D. K. Singh, "Shear characteristics of Lean Duplex Stainless Steel (LDSS) rectangular hollow beams structures", Vol. 10, pp. 13-29, 2017.
- [14] Z. Tao and K. J. R. Rasmussen, "Stress-Strain Model for Ferritic Stainless Steels", *J. Mater. Civ. Eng.*, Vol. 28, No. 2, 06015009, pp. 1-5, 2016.
- [15] M. Theofanous and L. Gardner, "Experimental and numerical studies of lean duplex stainless steel beams", *Journal of Constructional Steel Research*, Vol. 66, pp. 816-825, 2010.